



A method to compute absolute free energies or enthalpies of fluids

Friederike Schmid^a, Tanja Schilling^b

^a*Institut für Physik, Johannes Gutenberg Universität, Staudinger Weg 9, D55099 Mainz, Germany*

^b*Theory of Soft Condensed Matter, Université du Luxembourg, 162a, rue de la faïencerie, BRB0.07, 1511 Luxembourg*

Abstract

We propose a new method to compute the free energy or enthalpy of fluids or disordered solids by computer simulation. The main idea is to construct a reference system by freezing one representative configuration, and then carry out a thermodynamic integration. We present a strategy and an algorithm which allows to sample the thermodynamic integration path even in the case of liquids, despite the fact that the particles can diffuse freely through the system. The method is described in detail and illustrated with applications to hard sphere fluids and solids with mobile defects.

Keywords: simulation methods, liquids, phase equilibria

1. Introduction

The free energy or free enthalpy is a central quantity in the statistical physics and thermodynamics of equilibrium systems, and there has traditionally been large interest in computing free energies in many areas of science [1]. Free energies need to be evaluated if one wishes to locate first order phase boundaries accurately, to compare differently folded conformations of large molecules, or to characterize adsorption properties. In all of these cases, the quantities of interest are actually free energy *differences*, and a large number of elegant methods have been devised that allow to relate the free energies of specific systems with each other [2, 3, 4, 5, 6, 7, 8, 9]. An obvious alternative is to compute the absolute free energies of the two systems separately. Much less effort has been devoted to this type of approach. Computing the absolute free energies of arbitrary disordered or fluid systems such as, e.g., lipid membranes, solid with highly mobile defects, or nematic liquid crystals, remains one of the long-standing unsolved problems in computer simulations. If a fluid state has a direct connection with an ideal gas state in phase space, its free energy can be evaluated by standard thermodynamic integration techniques. In the systems mentioned above, however, the fluid phase of interest cannot be accessed from the gas phase in an obvious manner without crossing a first order phase boundary.

Here we propose a method to calculate the free energies of arbitrary liquids and disordered solids [10], which will hopefully contribute to solve the problem. The main idea is to freeze an arbitrary configuration in the phase of interest – a ‘representative’ configuration, obtained,

e.g., from a typical simulation of an equilibrated system – and to use this frozen ‘representative’ configuration as the reference system for a thermodynamic integration. This idea seems bold and precautions have to be taken to make it work for fluids. We propose an algorithm that allows to determine the free energies for simple fluids and solids (as we shall demonstrate for hard spheres), which can presumably be generalized to complex fluids in a fairly straightforward manner.

To put the method into context, we briefly sketch a few similar proposals in the past. Our idea is based on the “Einstein crystal” method originally developed by Frenkel and Ladd [11], which allows one to calculate the free energy of a regular crystal structure by establishing a thermodynamic integration path to a reference system where particles are pinned to the lattice sites of the same crystal by harmonic springs. This method has been generalized in various ways. For example, the “Einstein molecule” [12] method alleviates the practical difficulties associated with shifts of the whole crystal during a simulation, and an “Einstein well” method was designed for “cluster crystals” where the lattice sites are occupied by several particles [13]. Speedy has generalized the Einstein method for amorphous solids by proposing to use reference systems with irregularly distributed sites [14], much in the spirit of our ‘representative’ reference system.

The basic problem with applying the Einstein method to fluids is that “Einstein” particles are bound to their reference site – even in the limit of very weak springs – whereas fluid particles explore the whole space. In infinite space, the transition from the “Einstein” system to the free fluid is thus singular. In finite space, the singularity disappears, but sampling the relevant quantities for the thermodynamic integration remains difficult (see below). Tyka *et al* [15] have recently proposed to remedy this situation by using a complicated multi-particle spring potential, where particles are assigned to reference sites such that the *total* spring energy is minimal, under the constraint that there is still a one-to-one correspondence between particles and reference sites. Thus particles swap reference sites as they move along. As an application example, Tyka *et al* have calculated the free energies of liquid water and liquid argon. Their method has some similarities with the method we shall propose below, but our approach is conceptually simpler, and we do not need to solve a complex assignment problem for every single configuration.

Our paper is organized as follows. In the next two sections, we present first the basic strategy of our method, and then the practical implementation. Extensions of the method, e.g., to constant pressure pressure simulations, are discussed in Section 3. In Section 4, we present first results regarding the behavior of the algorithm for different algorithmic parameters, and applications to hard sphere fluids. We conclude and summarize in section 5.

2. Basic Strategy

For clarity, we will constrain the discussion to monatomic liquids at constant volume at first. Extensions, e.g., to constant pressure simulations will be introduced further below (Section 3). Furthermore, we only consider the configurational part of the free energy, since the kinetic part can be evaluated trivially [16]). The configurational energy is then characterized by a potential function or ‘Hamiltonian’ $U(\{\mathbf{r}_i\}) + H + 0$, which depends on the coordinates $\{\mathbf{r}_i\}$ of the particles i , and the configurational free energy shall be denoted F_0 .

The first step is to choose a ‘representative’ reference configuration, $\{\mathbf{r}_i^{\text{ref}}\}$, which is typically some arbitrary equilibrated configuration. The reference system is defined by the reference Hamiltonian

$$H_{\text{ref}}(\varepsilon) = \varepsilon \sum_i \Phi \left(\frac{|\mathbf{r}_i - \mathbf{r}_i^{\text{ref}}|}{r_{\text{cutoff}}} \right) + U(\{\mathbf{r}_i^{\text{ref}}\}) \quad , \quad (1)$$

where the function $\Phi(x)$ defines an attractive potential well with $\Phi(x) < 0$ for $x < 1$ and $\Phi \equiv 0$ elsewhere. The last term $U(\{\mathbf{r}_i^{\text{ref}}\})$ denotes the potential energy of hypothetical particles pinned to the *reference* sites and is thus constant. It is introduced for convenience. Note that there is formally a one-to-one correspondence between particles and reference sites, like in the Einstein crystal method. However, we want the particles to be indistinguishable (in the 'classical' sense), hence we allow them to swap identities (*i.e.*, labels i and j) during the simulation. This indistinguishability together with the finite range of the well potential (in the Einstein crystal, it is infinite) helps to avoid the conceptual problems with the transition between the reference system H_{ref} and the target system H_0 mentioned earlier. Moreover, we shall show below (Section 2.3) that the swap moves also speed up the equilibration times considerably. In the reference system, the particles do not interact directly with each other, hence its free energy $F_{\text{ref}}(\varepsilon)$ can be calculated analytically (see Section 2.1).

To establish the connection between the reference system H_{ref} and the target system H_0 , we introduce an intermediate model

$$H'(\lambda, \varepsilon) = H_{\text{inter}}(\lambda) + H_{\text{ref}}(\varepsilon) \quad (2)$$

that reduces to the target system H_0 at $(\lambda = 1, \varepsilon = 0)$ and to the reference system $H_{\text{ref}}(\varepsilon)$ at $\lambda = 0$. For example, one can choose $H_{\text{inter}}(\lambda) = \lambda \Delta U$ with $\Delta U := U(\{\mathbf{r}_i\}) - U(\{\mathbf{r}_i^{\text{ref}}\})$. Alternatively, a more complicated function like $H_{\text{inter}}(\lambda) = -k_B T \ln(1 - \lambda + \lambda e^{-\beta \Delta U})$ can be more convenient when dealing with hard core interactions. The free energy of the intermediate system (2) shall be denoted $F'(\lambda, \varepsilon)$. Within the intermediate model, we can construct a thermodynamic integration path connecting the reference and target system. In practice, it is often simplest to evaluate separately the free energy difference associated with switching on the particle interactions ($\lambda = 0 \rightarrow 1$) at fixed ε , and the free energy difference associated with switching off the well potentials in full presence of particle interactions ($\lambda = 1$). Other integration paths are also conceivable and may be more effective in some cases.

We will now discuss separately the different practical steps involved in this program.

2.1. Free energy of the reference system

We begin with calculating the free energy of the reference system. The partition function of a single particle in the volume V subject to a well potential $\Phi(|\mathbf{r} - \mathbf{r}^{\text{ref}}|/r_{\text{cutoff}})$ is given by

$$Q_1 = V + \int_V d\mathbf{r} \left[\exp(-\beta \varepsilon \Phi) - 1 \right] =: V + V_0 g_\Phi(\beta \varepsilon)$$

with $\beta = 1/k_B T$, where V_0 is the volume of a sphere with radius r_{cutoff} . This defines the function

$$g_\Phi(a) = \int_0^1 dx x^{d-1} [e^{-a\Phi(x)} - 1] \quad (3)$$

characterizing the effect of a well potential $\Phi(x)$ in d spatial dimensions on the single-particle partition function. Below, we shall mostly use a linear well potential,

$$\Phi(x) = \begin{cases} x - 1 & \text{for } x < 1 \\ 0 & \text{otherwise,} \end{cases} \quad (4)$$

giving

$$g_{\text{linear}}(a) = \frac{d!}{a^d} \left(e^a - \sum_{k=0}^d \frac{a^k}{k!} \right). \quad (5)$$

In terms of the characterizing function $g_\Phi(a)$, the configurational free energy of the reference system of N particles subject to the Hamiltonian $H_{\text{ref}}(\varepsilon)$ finally reads

$$F_{\text{ref}}(\varepsilon) = Nk_B T \left[\ln \left(\frac{N}{V} \right) - \ln \left(1 + \frac{V_0}{V} g_\Phi(\beta\varepsilon) \right) \right] + U(\{\mathbf{r}_i^{\text{ref}}\}). \quad (6)$$

2.2. Switching on the particle interactions

The next step consists in switching to the intermediate model $H'(\lambda, \varepsilon)$ and evaluating the free energy difference associated with taking the interaction parameter λ from zero to one. This could be done by a suitable thermodynamic integration. Here we will describe a different approach, which is also commonly used in the literature: We carry out a series of extended ensemble simulations where the parameter λ can switch between two values λ_0 and λ_1 (e.g., in the simplest case $\lambda_0 = 0$ and $\lambda_1 = 1$) by means of Monte Carlo trial moves, which are accepted or rejected according to a Metropolis criterion with the Hamiltonian $H'(\lambda, \varepsilon)$ (Equation (2)). The free energy difference of two systems with interactions $H_{\text{inter}}(\lambda_0)$ and $H_{\text{inter}}(\lambda_1)$ is then given by $\Delta F = F'(\lambda_1, \varepsilon) - F'(\lambda_0, \varepsilon) = -k_B T \ln(P_{\lambda_1}/P_{\lambda_0})$, where P_{λ_i} is the fraction of configurations with interaction parameter λ_i .

The question remains how to choose the steps λ_i . On the one hand, the free energy difference ΔF should not exceed several $k_B T$, otherwise the system stays in the more favorable state forever. On the other hand, it should not be too small, otherwise it becomes difficult to control the relative statistical error. By a simple argument, we can estimate that the 'optimal' free energy difference should be about $2 k_B T$:

Consider two systems with a total free energy difference ΔF_0 , and we have the task to evaluate the quantity $q = \exp(-\Delta F_0)$ by extended ensemble simulations of total length N . For simplicity, we assume that every Monte Carlo sweep results in an independent configuration. We compare two different simulation strategies: In the first, q is evaluated in one step within one single simulation run of length N , where the two systems are compared directly. In the second, q is evaluated in k steps, passing $(k - 1)$ intermediate system with free energies equally distributed between the two systems of interest. This involves k simulation runs of length N/k . In the first setup (one-step simulation), the fraction of configurations N_1 in the state of higher free energy is given by $N_1/N \sim \langle N_1/(N - N_1) \rangle = \exp(-\beta\Delta F_0)$ with the relative error $\Delta N_1/N_1 \approx \sqrt{1/N_1}$ (assuming Poisson statistics). Thus the simulation yields the quantity $q = \exp(-\beta\Delta F_0)$ with the relative error

$$\Delta q/q = \exp(\beta\Delta F_0/2) \cdot \sqrt{1/N}. \quad (7)$$

In the second setup, (k -step simulation), each simulation i ($i = 1, \dots, k$) gives a quantity $q_i = \exp(-\beta\Delta F_i)$ with the relative error $\Delta q_i/q_i = \exp(\beta\Delta F_i/2) \cdot \sqrt{k/N}$. Ideally, $\Delta F_i = \Delta F_0/k$ for all i , and the total relative error of $q = \prod_i q_i$ accumulates to

$$\Delta q/q = \exp(\beta\Delta F_0/2k) \cdot k/\sqrt{N}. \quad (8)$$

Comparing (7) and (8), one finds that a multi-step strategy is favorable as soon as the free energy difference ΔF_0 exceeds $4 \ln(2) \sim 2.77 k_B T$, and the optimal step size is characterized by a free energy difference of $\beta\Delta F_0/k = 2k_B T$.

2.3. Switching off the well potentials

Finally, in the last step, we gradually turn the well potentials to zero. We evaluate the free energy difference ΔF_2 between the intermediate model $H'(\lambda = 1, \varepsilon)$ and the target model $H'(\lambda =$

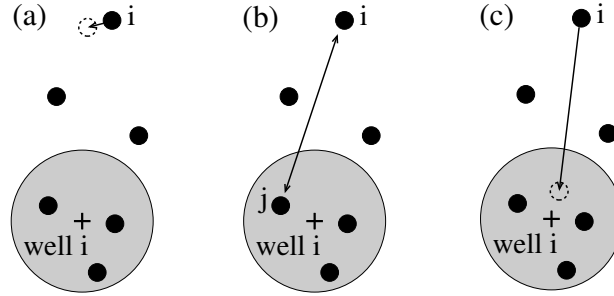


Figure 1: Sketch of moves in our Monte Carlo algorithm. (a) Simple particle displacements. (Could be replaced e.g., by short Molecular Dynamics runs.) (b) Smart particle swaps. (c) Smart particle relocations. See text for explanation

$1, \varepsilon = 0) = H_0$ by a thermodynamic integration, using

$$F_0 - F'(1, \varepsilon) = - \int_0^\varepsilon d\varepsilon' \left\langle \frac{\partial H'(1, \varepsilon')}{\partial \varepsilon'} \right\rangle_{\varepsilon'} = - \int_0^\varepsilon d\varepsilon' \left\langle \sum_i \Phi \left(\frac{|\mathbf{r}_i - \mathbf{r}_i^{\text{ref}}|}{r_{\text{cutoff}}} \right) \right\rangle_{\varepsilon'}. \quad (9)$$

Thus we need to sample the quantity $\langle \sum_i \Phi(|\mathbf{r}_i - \mathbf{r}_i^{\text{ref}}|/r_{\text{cutoff}}) \rangle$ on an integration path between $\varepsilon' = \varepsilon$ and $\varepsilon' = 0$. At this point, it becomes clear why our potential wells must have a finite range r_{cutoff} : If the wells had infinite range, sampling $\langle \Phi \rangle$ in fluids would be practically impossible in the limit $\varepsilon' = 0$, where the mean-square displacement of the particles diverges.

Setting a finite range for the reference potential, however, introduces a problem: The particles need to find their respective wells of attraction. We therefore introduce two Monte Carlo moves that help particles i explore their well i (Fig. 1). The first move (Fig. 1 b) swaps particles in a smart way and works as follows:

- Pick a random particle i and find the set of particles $\{n_i\}$ that are within the attraction range of well i .
- If particle $i \notin \{n_i\}$: pick a particle j from $\{n_i\}$, and swap i and j with the probability $\min\{1, \frac{n_i}{N} e^{-\Delta H'}\}$.
- Otherwise: pick a particle j from all particles
 - if $j \notin \{n_i\}$: swap with probability $\min\{1, \frac{N}{n_i} e^{-\Delta H'}\}$.
 - if $j \in \{n_i\}$: swap with probability $\min\{1, e^{-\Delta H'}\}$.

Here $\Delta H'$ is the difference of the energies (according to the intermediate model) of the old and new configuration. This algorithm promotes particle swaps that bring particles close to their respective well and nevertheless satisfies detailed balance.

The second move (Fig. 1 c) relocates particles i with a bias towards the neighborhood of their well i :

- Pick a random particle i (with position \mathbf{r}_i).
- Choose a new position \mathbf{r}'_i from a given (biased) distribution $P_i(\mathbf{r}'_i) = \exp(-W(|\mathbf{r}'_i - \mathbf{r}_i^{\text{ref}}|))$.
- Relocate the particle from \mathbf{r} to \mathbf{r}'_i with probability $\min\{1, P(\mathbf{r}_i)/P(\mathbf{r}'_i) e^{-\Delta H'}\}$.

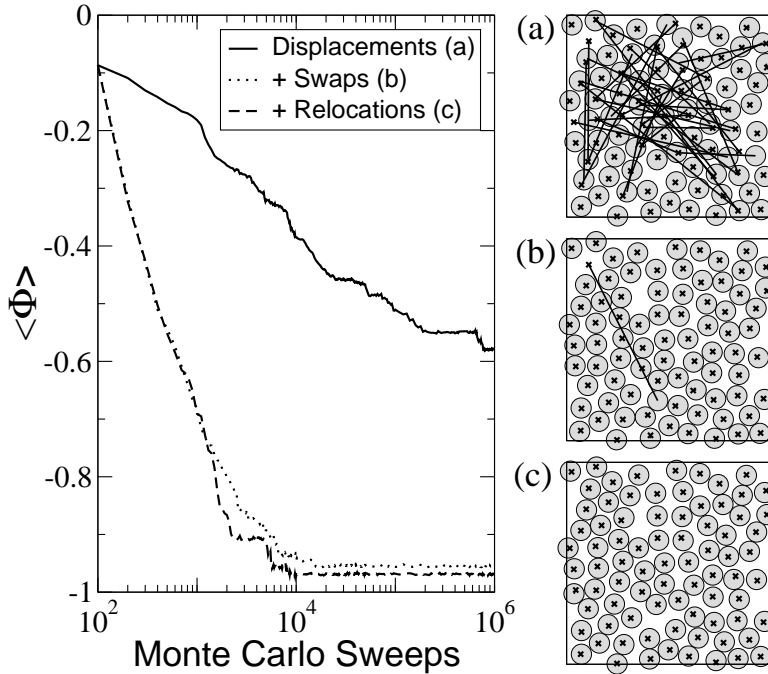


Figure 2: Illustration of the effect of the moves of Fig. 1 on the equilibration of a system of 80 hard disks (diameter D) at a density $\rho = 0.8/D^2$, after switching on linear well potentials with strength $\varepsilon = 50k_B T$ ($r_{\text{cutoff}} = 2D$). Swap moves and relocation moves (one per bead) were attempted one per 100 MC sweeps. Left: Evolution of $\langle \Phi \rangle$ in simulations that include different moves as indicated. Right: Corresponding final configurations. Circles indicate particle positions, crosses give well positions. Particles and their respective wells are connected by straight lines. See text for more explanation. From Ref. [10].

Obvious choices for $W(r)$ which we have tested are $W(r) = \varepsilon\Phi(r/r_{\text{cutoff}})$, or $W(r) = \text{const.}$ for $r < r_{\text{cutoff}}$. As long as the wells are weak (low ε'), the relocation moves have little effect. At high ε' , they help to overcome trapped situations where most particles are bound to a well, and a few cannot escape from a local cage.

The effect of the different moves is shown in Fig. 2 (taken from Ref. [10]). It shows the evolution of the observable $\langle \Phi_i \rangle$, averaged over all particles i , in a two dimensional system of hard disks (diameter D) at packing fraction $\eta = 0.63$, after ε had been raised from zero to $\varepsilon = 50k_B T$. The well potential is linear (Eq. (4)) with range $r_{\text{cutoff}} = 2D$. In a Monte Carlo simulation that includes only random particle displacements, the system is still far from equilibration after one million MC sweeps (a). Smart swap moves (one per 100 Monte Carlo sweeps) speed up the equilibration by orders of magnitude, but the system gets trapped in a configuration where one particle remains separated from its well (b). This problem is solved by including smart relocation moves (c).

3. Extensions of the method

The algorithm described above can easily be generalized to molecular fluids: one must simply swap molecules instead of particles (atoms). To generalize it to free enthalpy calculations (systems at constant pressure), we employ a reference system that is defined in terms of scalable coordinates, *i.e.*, the reference sites are rescaled along with the particle coordinates if the volume of the system changes. Furthermore, the volume V of the system is pinned to the reference volume by an additional term $\varepsilon(V - V_{\text{ref}})^2$ in the reference Hamiltonian. We can then follow the strategy described above, with two modifications: First, the derivative of the free energy in Equation (9) has an additional contribution

$$\frac{\partial F'}{\partial \varepsilon} = \left\langle \frac{\partial H'}{\partial \varepsilon} \right\rangle = \left\langle \sum_i \Phi \left(\frac{|\mathbf{r}_i - \mathbf{r}_i^{\text{ref}}|}{r_{\text{cutoff}}} \right) \right\rangle + \langle (V - V_{\text{ref}})^2 \rangle. \quad (10)$$

Second, the expression for the free enthalpy of the reference system changes. In practice, the fluctuations of the volume V become negligible already at moderate ε , ($\varepsilon > 10k_B T$ in our case), such that the reference free energy can be written as

$$\frac{\beta G_{\text{ref}}(\varepsilon)}{N} = \frac{PV_{\text{ref}}}{N} - 1 + \ln \left(\frac{N}{V_{\text{ref}}} \right) - \ln \left(1 + \frac{V_0}{V_{\text{ref}}} g_{\Phi}(\beta \varepsilon) \right) \quad (11)$$

to a very good approximation.

4. Results

4.1. Transition to the reference state: Effect of well shape and well range

Before presenting our first real application examples, we will discuss a few properties of the algorithm at the example of the two-dimensional ideal gas. Figure 3 illustrates the influence of the shape and range of the well potential. Three well shapes are compared, the (most popular) harmonic well, the linear well (Equation (4)), and a "square root" well with the shape $\Phi(x) = \sqrt{x} - 1$. The top panel in Figure 3 demonstrates that of these three potentials, the harmonic well is most effective in trapping the particles for small and moderate ε . All three potentials however bind almost 100 % of all particles for $\varepsilon > 20k_B T$. At higher ε , the linear and the square root potential localize the particles much better (lowest panel in Figure 3), which makes it more easy to switch on interactions (step 2.2) in the case of interacting particles. The middle panel in Figure 3 shows the averaged well energy per particle $\langle \Phi \rangle / N$, *i.e.*, the quantity that needs to be sampled for the thermodynamic interactions. It is remarkable that $\langle \Phi \rangle / N$ is still noticeably different from its limiting value ($\langle \Phi \rangle / N = 1$) even for ε -values as high as $\varepsilon = 50k_B T$. Despite the fact that it localizes particles most efficiently, the square well potential reaches the limiting value more slowly than the other potentials. In the following studies, we will mostly settle on using linear well potentials.

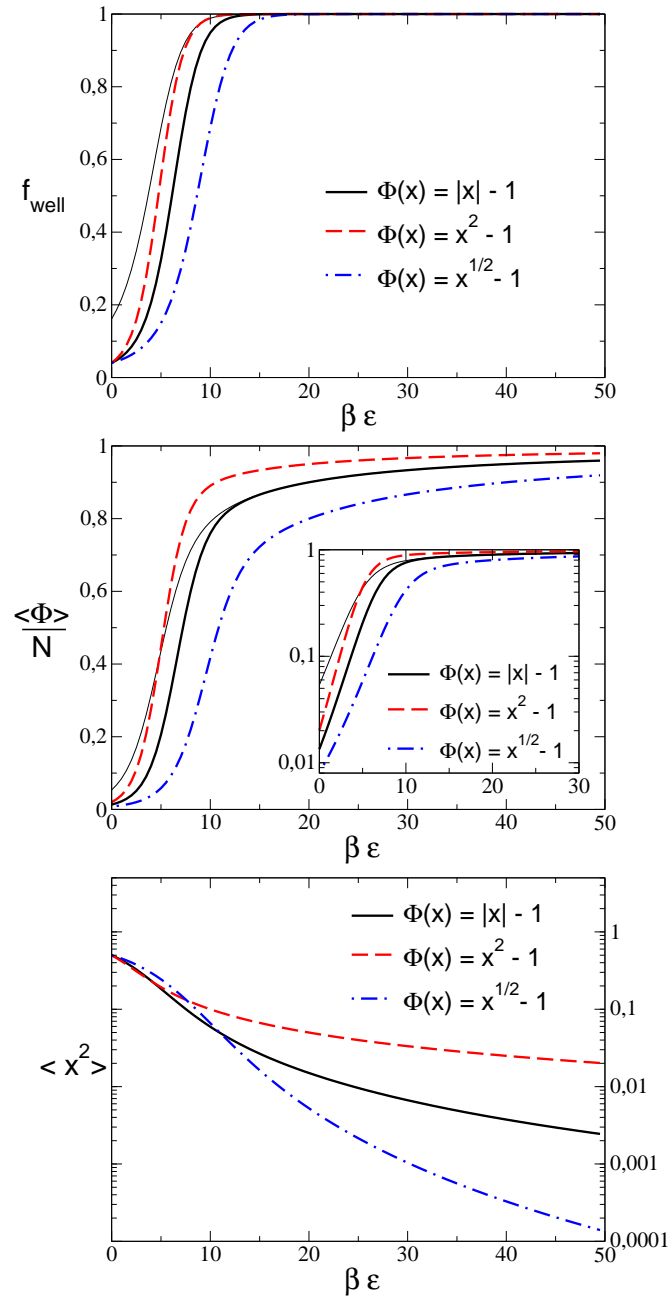


Figure 3: Effect of well shape $\Phi(x)$ on the behavior of different quantities as a function of well strength ϵ in the two dimensional ideal gas. Top: Fraction f_{well} of particles inside the well. Middle: Free energy derivative per particle $\langle\Phi\rangle/N. = -\partial F/\partial\epsilon \cdot N^{-1}$. Bottom: Mean-square displacement of those particles that are within the well range. Dashed line corresponds to a quadratic well, thick solid line to a linear well, and dot-dashed line to a square root well with well range σ . The thin solid line shows the behavior of the same quantities for a linear well with range 2σ for comparison. The volume is $V = 77.94\sigma^2$ (Here σ is an arbitrary length scale).

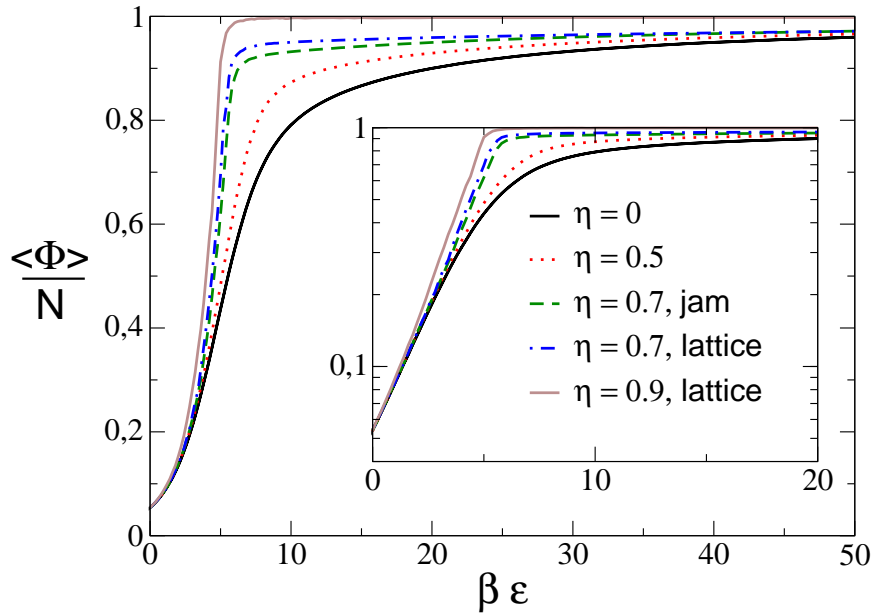


Figure 4: Free energy derivative per particle $\langle \Phi \rangle / N = -\partial F / \partial \epsilon \cdot N^{-1}$ in a system of hard disk particles with different diameters, *i.e.*, different packing fractions η . The shape of the well potential is linear with cutoff $r_{\text{cutoff}} = 2\sigma$. The other parameters are the same as in Fig. 3.

4.2. Transition to the reference state: Effect of packing fraction

Next we study the effect of particle interactions. To this end, we introduce hard disk interactions in the system of Figure 3 (using the linear well potential with range $r_{\text{cutoff}} = 2\sigma$). By adjusting the disk radius, we vary the packing fraction η between $\eta = 0$ and $\eta = 0.9$, which is close to the maximum value $\eta_{\text{max}} = 0.9069$. At the two higher packing fractions, $\eta = 0.7$ and $\eta = 0.9$, the stable state is an ordered crystal structure. At $\eta = 0.7$, we also show for comparison the curve obtained with a (metastable) disordered reference state.

With increasing packing fraction, the particles settle more rapidly in their respective wells. This also happens faster for the ordered system than for the jammed system. To check for hysteresis effects, the curves were sampled in both directions, with *i.e.*, increasing and decreasing ϵ . We did not encounter any signs of a first order transition. At the highest packing fraction $\eta = 0.9$, the equilibration times were found to become very large for small ϵ . The reason is that in the absence of wells, the center of gravity of the whole crystalline system diffuses around very slowly. This problem is already well known from the 'Einstein crystal' method and has led to the development of the 'Einstein molecule' method, where the reference system is defined in terms of relative coordinates rather than absolute coordinates [12]. The same idea can also be used here.

4.3. Application: Hard sphere fluids

After these more technical discussions, we turn to presenting real applications. As a first application example, we have determined the absolute free energies of systems of 256 hard spheres with diameter D at the densities $N/V = 0.25D^{-3}$, $0.5D^{-3}$, and $0.75D^{-3}$. The results can be compared with those obtained by integration of the Carnahan-Starling equation-of-state[17], which describes the behavior of three dimensional hard sphere fluids very accurately. To obtain the free energies, we have used 50 values of ε and 6×10^5 Monte Carlo sweeps for each data point for the two lower densities, and 200 values of ε times one million Monte Carlo sweeps for the density $0.75D^{-3}$. The results are given in Table 1. Within the error, all results agree well with the theoretical value from the Carnahan-Starling equation.

For the density $0.5D^{-3}$ (corresponding to a liquid state), we compared three different situations: (a) linear well Φ and liquid reference state, (b) linear well Φ and crystalline reference state, (b) harmonic well Φ and liquid reference state. All variations gave the same results. In case (b), we did not see a hysteresis on increasing/decreasing ε – apparently, the trapping of particles in a crystalline array of wells is not associated with a phase transition at this density. We expect that this will be different closer to the liquid/solid transition. Nevertheless, we can conclude that our method is robust and may work if the reference configuration is not really representative for the target structure. Comparing the calculation for linear and harmonic wells, we find that the result also does not depend on the shape of the well. However, for more accurate potential, the linear potential seems to be more useful, because the particles get trapped more efficiently.

Table 1: Results for the free energy of hard spheres (from Ref. [10]). F/N_{CS} is the value according to the Carnahan-Starling equation-of-state [17]. a) linear potential Φ , liquid reference state. b) linear Φ , hcp reference state. c) harmonic Φ , liquid reference state.

N/V	F/N	$(F/N)_{CS}$
0.25	0.620 ± 0.002	0.625
$0.5^a)$	1.541 ± 0.002	1.544
$0.5^b)$	1.540 ± 0.002	1.544
$0.5^c)$	1.549 ± 0.002	1.544
0.75	3.009 ± 0.005	3.005

4.4. Free energy of a vacancy

Our last example shows an application of the method to a dense disordered system, where the dynamics is driven by cooperative processes. We have studied hard disks (two dimensions, diameter D) up to densities where the equilibrium state is solid, and enforced a vacancy defect by taking one particle out of an otherwise ordered configuration. To calculate the free energy of the vacancy, we must compare the *enthalpy* of this system with that of an ordered system at the same pressure. Thus simulations were carried out at constant pressure (see Section 3) in a rectangular simulation box of varying area and fixed side ratio $1 : \sqrt{3}/4$. The vacancy is then stable, but highly mobile (Figure 5, top right).

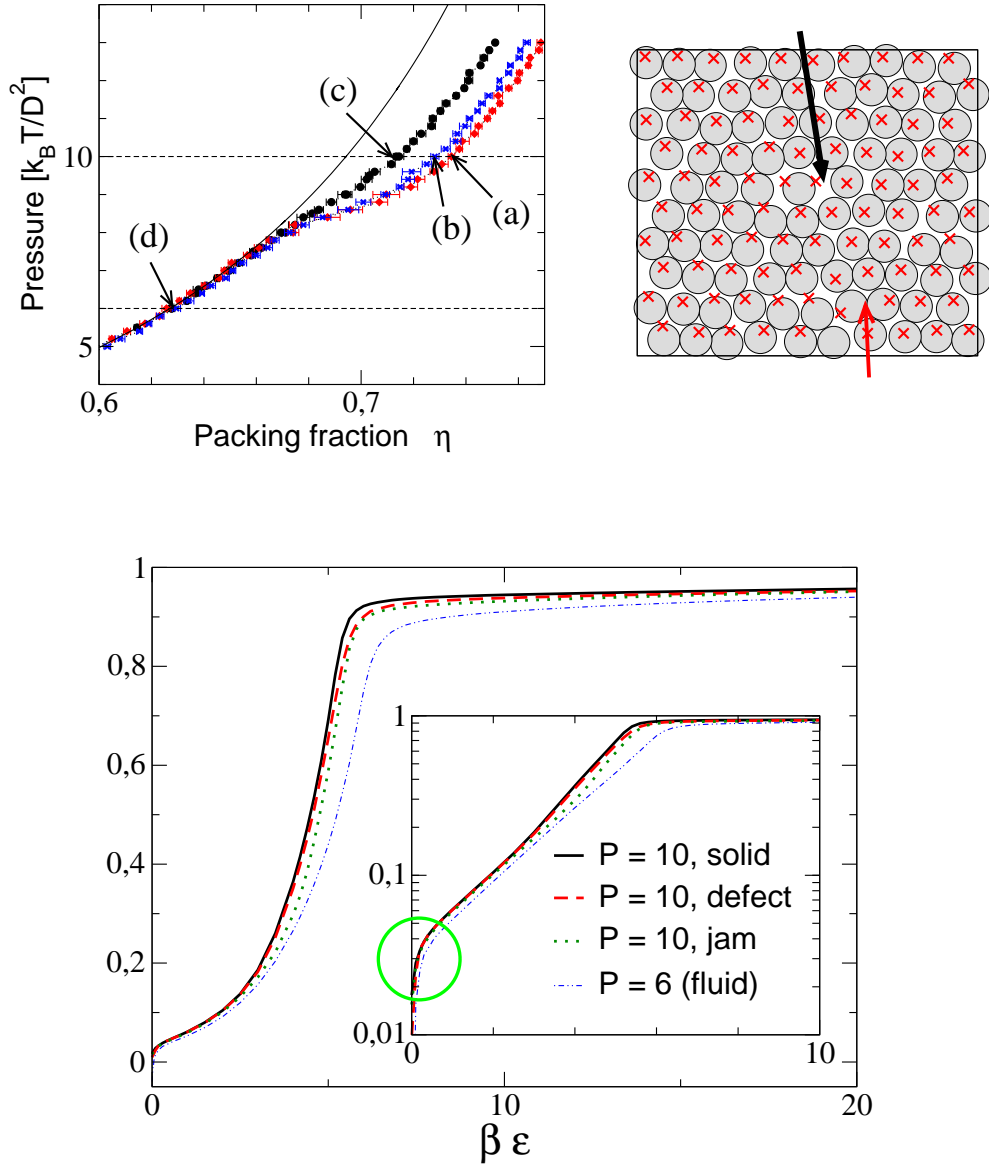


Figure 5: Free enthalpy calculations of dense hard-disk systems (diameter D). Top left: Pressure vs. packing fraction as obtained from constant pressure simulations at $\epsilon = 0$. (a) expanded from an ordered solid phase, (b) expanded from a solid phase with one vacancy, (c) compressed from the fluid phase. The solid line shows the theoretical estimate [18] $P = \hat{\rho}/(1 - \hat{\rho} \cdot \pi/4)^2$ with $\hat{\rho} = (N + 1)/\langle V \rangle$. Top right: Configuration snapshots with one vacancy at the beginning (crosses) and the end (circles) of a Monte Carlo run at $\epsilon = 0$. The arrows mark the position of the defect in the two cases, illustrating its high mobility. Bottom: Derivative $-\partial F/\partial \epsilon$ of the free energy along the path of thermodynamic integration for the three dense systems (a), (b), and (c) at pressure $P = 10k_B T/D^2$, and for a fluid system at $P = 6k_B T/D^2$. The inset shows the same data in a semi-logarithmic scale. The circle highlights the area where the volume fluctuations contribute noticeably to $\partial F/\partial \epsilon$.

We compare four different structures (Figure 5): An ordered solid (a), an ordered solid with a vacancy (b), and for comparison also a metastable disordered jammed state (c), which was obtained by compressing the system from the fluid state, and a fluid state (d) at lower pressure. Figure 5 (top left) shows the corresponding pressure-density curves of the target system ($\varepsilon = 0$). Free enthalpy calculations were carried out at $P = 10k_B T/D^2$ for the three cases (a-c), and at $P = 6k_B T/D^2$ for the case (d). The resulting free enthalpies can be related to the chemical potential μ by virtue of the thermodynamic relation $G = \mu N$. Figure 5 shows the corresponding evolution of the integrands $\langle \partial H' / \partial \varepsilon \rangle$ of the thermodynamic integration (Equation (10)) up to $\varepsilon = 20$. (in total, ε was varied between 0 and $50k_B T$). The volume fluctuations contribute only for very small ε . The curves for the jam, solid, and defect state are slightly different, reflecting the differences in the free enthalpies of the different states.

At $P = 6k_B T/D^2$, the free enthalpy calculation yields the chemical potential $\mu = 8.997 \pm 0.002k_B T$, which is in good agreement with the theoretical estimate of Helfand *et al* [18] $\mu = 9.047k_B T$. At $P = 10k_B T/D^2$, we find $\mu_{\text{solid}} = 13.617 \pm 0.002k_B T$ in the solid state, and $\mu_{\text{jam}} = 13.675 \pm 0.002k_B T$ in the jammed state, which establishes that the solid state is indeed the stable phase. For the system with one defect, we obtained the total enthalpy $G_{\text{defect}} = 1361.7 \pm 0.2k_B T$. This result can be used to estimate the core free energy of the vacancy $\mu_c = G_{\text{defect}} - \mu_{\text{solid}}N + k_B T \ln(N) = 7.1 \pm 0.3k_B T$, which corresponds to a relative vacancy frequency of roughly 10^{-3} . (For comparison, the frequency of vacancies at liquid/solid coexistence in three dimensions is roughly 10^{-4} , according to Pronk *et al* [19]). Since finite size effects stabilize the defect, μ_c is probably largely overestimated, hence the value given above has to be interpreted as an upper bound. More detailed studies shall be carried out in the future. Here, the example mainly serves to illustrate the use of our approach in situations where free energies are difficult to access with other methods.

5. Conclusions

In summary, we propose a new method to compute absolute free energies for fluids, liquids, and disordered structures. The method generalizes the Einstein crystal method of Frenkel and Ladd [11], but can be applied much more widely. We anticipate that the method will be useful for studies of complex fluids and biological systems, *e.g.*, proteins in solution. This remains to be tested. The method has recently been published [10], and a few application examples have been given. We hope that the detailed discussion in the present proceedings paper will motivate researchers to try and apply the method to many other systems and further explore its potential.

References

- [1] C. Chipot and A. Pohorille, eds., *Free energy calculations: Theory and applications in chemistry and biology* (Springer Verlag, Berlin, 2007).
- [2] D. Frenkel, B. Smit, *Understanding molecular simulation* (Academic Press, London, 2002).
- [3] D. P. Landau, K. Binder, *A guide to Monte Carlo simulations in Statistical Physics* (Cambridge University Press, 2005).
- [4] D. Earl, M. Deem. Phys. Chem. Chem. Phys. **7**, 3910 (2005).
- [5] Y. Okamoto, Journal of Molecular Graphics and Modelling **22**, S1425 (2004).
- [6] A. Panagiotopoulos, J. Phys.: Cond. Matt. **12**, R25 (2000).
- [7] J. de Pablo, Q. Yan, F. Escobedo, Ann. Rev. Phys. Chem. **50**, 377 (1999).
- [8] A. D. Bruce, A. N. Jackson, G. J. Ackland, N. B. Wilding, Phys. Rev. E **61**, 906 (2000).
- [9] N. B. Wilding, A. D. Bruce, Phys. Rev. Lett. **85**, 5138 (2000).
- [10] T. Schilling, F. Schmid, J. Chem. Phys. **131**, 231102 (2009).

- [11] D. Frenkel, A. Ladd, J. Chem. Phys. **81**, 3188 (1984).
- [12] C. Vega, E. Noya, J. Chem. Phys. **127**, 154113 (2007).
- [13] B.M. Mladek, P. Charbonneau, C.N. Likos, D. Frenkel, G. Kahl, J. Phys: Cond. Matter **20**, 494245 (2008).
- [14] R.B. Speedy, Mol. Phys. **80**, 1105 (1993).
- [15] M.D. Tyka, R.B. Sessions, A.R. Clarke, J. Phys. Chem. B **111**, 9571 (2007).
- [16] R. Jellitto, *Thermodynamik und Statistik* (Aula Verlag, Wiesbaden, 1989).
- [17] N. Carnahan, K. Starling, J. Chem. Phys. **51**, 635 (1969).
- [18] E. Helfand, H.L. Frisch, J.L. Lebowitz, J. Chem. Phys. **34**, 1037 (1960).
- [19] S. Pronk, D. Frenkel, J. Phys. Chem. B **105**, 6722 (2001).